Geoscience Canada

U-Pb Geochronology Using 193 nm Excimer LA-ICP-MS Optimized for *In Situ* Accessory Mineral Dating in Thin Sections

Chris R.M. McFarlane and Yan Luo

Volume 39, Number 3, 2012

URI: https://id.erudit.org/iderudit/geocan39_3maf01

See table of contents

Publisher(s)

The Geological Association of Canada

ISSN

0315-0941 (print)
1911-4850 (digital)

Explore this journal

Cite this article

McFarlane, C. R. & Luo, Y. (2012). U-Pb Geochronology Using 193 nm Excimer LA-ICP-MS Optimized for *In Situ* Accessory Mineral Dating in Thin Sections. *Geoscience Canada*, *39*(3), 158–172.

Article abstract

This article is designed to provide a synopsis of the application of LAICP-MS to U-Pb geochronology of accessory minerals, in standard polished thin sections, using modern 193 nm ArF excimer laser ablation (LA) and quadrupole inductively coupled plasma mass spectrometry (Q-ICP-MS) instrumentation. During about the last five years, Q-ICP-MS manufacturers (e.g. Agilent, Thermo Scientific, Perkin Elmer, Bruker Daltonics) have introduced new instruments or interfaces with higher sensitivity and lower backgrounds, compared to the previous generation of instruments. ArF excimer laser systems built by Resonetics (RESOlution™ M-50 and S-50), NewWave Research (NWR-193™), Photon Machines (Excite™ and Analyte G2™), and Coherent (GeoLas™), have also expanded their capabilities in a relatively short period of time. There has also been a significant leap in software development and laser control, which, when matched with sophisticated offline data processing has increased the overall efficiency of the technique.

This article begins with a background section designed to provide the basic bibliography and theory of laser-target interaction for nanosecond and femtosecond lasers. We then describe enhancements in ICP-MS sensitivity, the importance of the laser-ablation cell, smoothing devices, and synchronized hardware and software controls. We also provide examples of how these recent advances have dramatically increased the efficiency (e.g. cost per analysis), precision and accuracy of *in situ* U-Pb geochronology of accessory minerals using 193 nm excimer LA-ICP-MS. Demonstration datasets are based on the instrumentation installed at the University of New Brunswick, and provide examples of the general capabilities of excimer LAICP-MS for detailed *in situ* U-Pb geochronology.

Modern Analytical Facilities

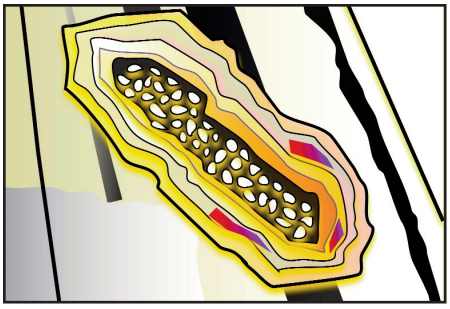

U-Pb Geochronology Using 193 nm Excimer LA-ICP-MS Optimized for *In Situ* Accessory Mineral Dating in Thin Sections

Chris R.M. McFarlane* and Yan Luo
Department of Earth Sciences, University of New Brunswick, Fredericton, NB, Canada E3B 5A3
crmm@unb.ca and yanluo@unb.ca

**Corresponding Author*

SUMMARY

This article is designed to provide a synopsis of the application of LA-ICP-MS to U-Pb geochronology of accessory minerals, in standard polished thin sections, using modern 193 nm ArF excimer laser ablation (LA) and quadrupole inductively coupled plasma mass spectrometry (Q-ICP-MS) instrumentation. During about the last five years, Q-ICP-MS manufacturers (e.g. Agilent, Thermo Scientific, Perkin Elmer, Bruker Daltonics) have introduced new instruments or interfaces with higher sensitivity and lower backgrounds, compared to the previous generation of instruments. ArF excimer laser systems built by Resonetics (RESOlution™ M-50 and S-50), NewWave Research (NWR-193™), Photon Machines (Excite™ and Analyte G2™), and Coherent (GeoLas™), have also expanded their capabilities in a relatively short period of time. There has also been a significant leap in software development and laser control, which, when matched with sophisticated offline data processing has increased the overall efficiency of the technique.

This article begins with a background section designed to provide the basic bibliography and theory of laser-target interaction for nanosecond and femtosecond lasers. We then describe enhancements in ICP-MS sensitivity, the importance of the laser-ablation cell, smoothing devices, and synchronized hardware and software controls. We also provide examples of how these recent advances have dramatically increased the efficiency (e.g. cost per analysis), precision and accuracy of *in situ* U-Pb geochronology of accessory minerals using 193 nm excimer LA-ICP-MS. Demonstration datasets are based on the instrumentation installed at the University of New Brunswick, and provide examples of the general capabilities of excimer LA-ICP-MS for detailed *in situ* U-Pb geochronology.

SOMMAIRE

Le présent article constitue un abrégé sur l'application de la spectroscopie de masse à plasma inductif à ablation par laser (ICP-MS) à la géochronologie U-Pb des minéraux accessoires en plaques minces polies normales, en utilisant une version moderne d'un laser excimère ArF d'ablation avec la spectrométrie de masse quadripolaire à plasma à couplage inductif (Q-ICPMS). Au cours des cinq dernières années environ, les manufacturiers de Q-ICPMS (Agilent, Thermo Scientific, PerkinElmer, Bruker Daltonics, par exemple) ont présenté de nouveaux instruments ou interfaces de meilleure sensibilité et de moindre bruit de fond par rapport aux générations d'instrument précédentes. Les systèmes laser excimère ArF construits par Resonetics (RESOlution^{MC} M-50 et S-50), newWave Research (NWR-193^{MC}), Photon Machines (Excite^{MC} et AnalyteG2^{MC}), et Coherent (GeoLas^{MC}) ont eux-aussi amélioré leurs capacités dans une période relativement courte. Il y a également eu une avancée significative dans le développement de logiciels et de contrôle du laser, ce qui, combiné à des traitements de données hors ligne sophistiqués a augmenté l'efficacité globale de la technique.

Cet article commence par un rappel de la bibliographie de base et de la théorie de l'interaction laser-cible pour les lasers nanosecondes et femtosecondes. Nous traitons ensuite des améliorations de sensibilité de l'ICP-MS, de l'importance de la cellule d'ablation par laser, des dispositifs de lissage, et des contrôles synchronisés matériels et logiciels. Nous donnons également des exemples de la façon dont ces progrès récents ont considérablement augmenté l'efficacité (par exemple le coût par analyse), la précision et l'exactitude de la géochronologie U-Pb *in-situ* sur minéraux accessoires par ICP-MS à ablation par laser excimère 193 nm. Les jeux de données de la démonstration qui proviennent de l'instrumentation installée à l'University of New Brunswick, donnent des exemples des capacités générales de l'ICP-MS à ablation par laser excimère pour l'analyse géochronologique U-Pb *in situ*.

INTRODUCTION

There are numerous landmark references that chronicle LA-ICP-MS development and applications to U-Pb geochronology. Most of these are referenced in two Mineralogical Association of Canada Short Course Series (volumes 29 and 40; (Sylvester 2001; Sylvester 2008) . These provide historical perspectives and a thorough treatment of LA-ICP-MS analytical techniques and applications. More recently, a wide variety of studies have appeared in such journals as the Journal of Analytical Atomic Spectrometry (JAAS), Analytical Chemistry, Applied Spectroscopy, and Chemical Geology. A recent Open Access (OA) review by Koch and Gunther (2011) also provides a useful 'state-of-the-art' review, including some remarks on the design and performance of sampling cells and the relative merits of femtosecond laser systems:

http://www.ingentaconnect.com/content/sas/sas/2011/00000065/00000005/art00006.

Other review papers include those of Cocherie and Robert (2008) who review laser ablation zircon U-Pb dating compared to ion-microprobe techniques, and Becker (2002), who provides a good review of the intrinsic accuracy, precision, and mass discrimination behaviour of plasma-source mass spectrometers. The University of Arizona Laserchron facility also provides a wealth of information about U-Pb dating techniques applicable to a wide range of accessory minerals:

https://sites.google.com/a/laserchron.org/laserchron/home.

Studies focusing on zircon dating by LA-ICP-MS are plentiful, but recent studies of allanite (Pal et al. 2011; Darling et al. 2012; Gregory et al. 2012), apatite (Chew et al. 2011), xenotime (Liu et al. 2011), and rutile (Zack et al. 2011) have greatly extended the range of dateable accessory minerals and associated host rock types.

There has been a recent proliferation of 193 nm ArF excimer LA-ICP-MS systems in Earth Sciences departments across Canada. Systems have recently been installed (or are due to be installed) at: University of New Brunswick (source of data for this paper), Université de Québec à Chicoutimi, University of Ottawa, the Geological Survey of Canada in Ottawa, Laurentian University, University of Alberta, and the University of British Columbia. Some of these systems are tailored to suit a particular research focus so potential users need to assess whether the instrumentation is capable of carrying out their desired analyses.

Potential users should also be aware of the cost involved with LA-ICP-MS projects. The most significant consumable costs are associated with consumption of high-purity gases: 1) the ICP-MS torch and Ar carrier gas together typically consume Ar at a rate of 18 to 20 L/min; 2) He used as a carrier gas is consumed at between 0.5 to 1.0 L/min; 3) the ArF premix used to create 193 nm laser pulses needs to be replenished approximately every two weeks depending on laser usage; and 4) low-grade N_2 used for laser beam line purge is consumed at 5 L/min when the laser is in operation. Taken together, yearly gas consumption for excimer LA-ICP-MS facilities is about $25–30K. Other consumables include valuable reference materials, Hg traps, polishing supplies, ICP-MS consumables (e.g. torch, sampler, skimmer and detector), cleaning supplies, tubing, vacuum pump consumables, etc. Additional costs are associated with salary recovery for technician time and yearly maintenance and repair bills for both the laser and ICP-MS. Thus, the actual cost of running a LA-ICP-MS facility can be quite high (up to ~ $100K/year) and so lab fee structures reflect this large consumable burden. Nonetheless, the productivity of LA-ICP-MS still makes this technology the most cost effective dating technique that exists today

Fundamentals of Laser-ablation

There are currently two types of laser ablation systems being used for U-Pb geochronology: 1) nanosecond (ns) lasers (common); and 2) femtosecond (fs) lasers (currently rare).

The first type includes 266 nm, 213 nm, and 193 nm lasers. The exact mechanism used to generate ns-laser pulses of a specific wavelength and energy is discussed elsewhere (e.g. Basting and Marowsky 2005). It is worth noting, however, that 193 nm excimer (i.e. '*exc*ited-d*imer*') lasers are generated using an ArF gas (the 'premix'), which, when pumped above its ground state results in photon emission at a 193 nm fundamental frequency. This means that in contrast to solid-state Nd:YAG laser sources, no complex optical quintupling methods are necessary and this greatly simplifies the optical design and maintenance of 193 nm ArF excimer laser systems. Excimer laser pulses have higher energy density compared to 266 nm and 213 nm UV lasers and by varying laser operating conditions and using optical attenuators, 193 nm excimer lasers can deliver a wide range of fluences (<1 to 40 J/cm^2) to the target. This wide dynamic range is necessary because ablation thresholds depend strongly on the composition of the target (i.e. absorption, electrical conductivity). For example, controlled ablation of translucent apatite typically requires fluence >10 J/cm^2 whereas zircon, monazite, and titanite can be ablated over a range of fluences (2 to 8 J/cm^2) that can be fine tuned to achieve an ablation rate (e.g. 0.5 μm/s) suitable for *in situ* analyses in polished thin sections.

Whatever the ns-laser source, the energy contained in each pulse is transferred into the target lattice over ns-timescales. When the energy of the laser pulses exceeds a target's ablation threshold, the solid's binding energy is overcome causing it to thermally decompose into a mixture of atoms, ions, and fragments. The particle size distribution generated by ns-LA-ICP-MS peaks in the range of 60 to 100 nm, and 193 nm ArF excimer lasers typically generate fewer μm-scale fragments, compared to 213 nm and 266 nm wavelengths (Guillong et al. 2003). The short timescales for interaction of the incoming pulse (e.g. between 4 ns and 20 ns for excimer lasers) allows most of the energy to be absorbed within the target area. Nonetheless, the target area is subject to *zone heating* that can cause preferential evaporation of volatile elements, such as Pb. This ablated material rapidly expands into a transient plasma plume above the target area. This plume interacts with subsequent laser pulses in a process known as *plasma shielding* which further alters the size and composition of the

aerosol. Outer-shell electron transitions in the plasma plume also release photons with wavelengths characteristic of the elements present in the plume. This is the basis of laser-induced breakdown spectroscopy (LIBS).

The net result of these thermally activated laser-target interaction processes is 'non-stoichiometric' ablation and the occurrence of elemental fractionation. For U-Pb geochronology applications, this element fractionation is manifested as increasing Pb/U as craters deepen. Eggins et al. (1998) have elegantly demonstrated and described the processes occurring at the ablation site that give rise to this laser-induced elemental fractionation (LIEF). This study revealed the presence of a volatile-element-enriched condensate blanket surrounding ablation craters and related its formation to condensation of volatile elements (e.g. Pb) out of the expanding plasma plume. Figure 1 shows a typical condensate blanket surrounding craters in zircon analysed by the UNB laser ablation system. This observation suggests that heavier elements with greater inertia are actually preferentially entrained in the carrier gas so that some other process must account for the observed increase in Pb/U as a function of time during ablation of craters. Careful inspection of craters by Eggins et al. (1998) revealed, however, that heavier refractory elements (e.g. U) appear to be preferentially deposited (e.g. by vapour deposition) on the inner walls of the craters as the plasma plume expands from progressively deeper into the material. Their results also suggest that whereas the ablation process is quantitative for shallow craters (i.e. most of the laser interaction volume is converted to aerosol), deep craters (i.e. depth/diameter >>1) are subject to plasma re-sampling and re-deposition that prevents a large fraction of the ablated volume from becoming aerosolized and entrained in the carrier gas.

These are some of the characteristics of ns-laser ablations systems that cause Pb/U fractionation resulting from laser–target interactions in drilling mode. The following movies available on YouTube demonstrate how three laser operating conditions

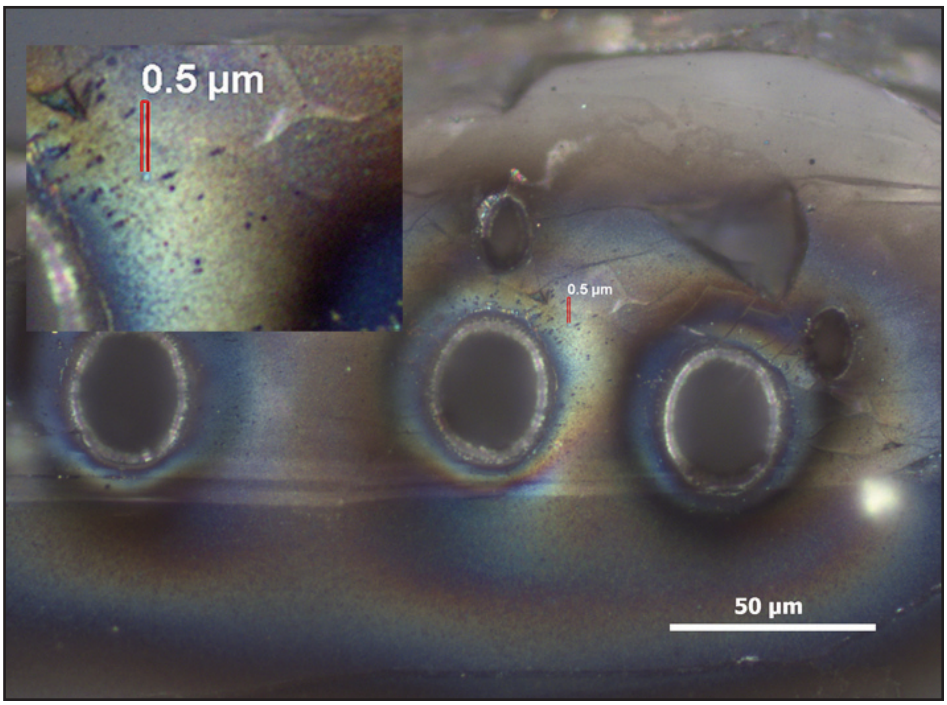

Figure 1. Reflected light photomicrograph (Zeiss AxioImager, 50 x objective) of ablation blankets surrounding 33 µm diameter craters in zircon. The largest particles visible are ~500 nm in size. The majority of the blanket is composed of much finer particles (<100 nm) that are just barely resolvable optically. This blanket is presumably formed from volatile-enriched nanoscale-particles that have condensed out of the expanding plasma plume. The particle size fraction carried away by the in-cell carrier gas is expected to be <100 nm.

(19 µm crater @ 10 Hz, 26 µm crater @ 5 Hz, and 45 µm crater @ 4 Hz) can influence the time-dependent increase in $^{206}Pb/^{238}U$ during ablation of zircon 91500 standards:

http://youtu.be/OLYwy7VQKgU
http://youtu.be/HOh8MMFMZOw.

In contrast, femtosecond laser pulses transfer energy to a material in a fundamentally different way. Rather than being a thermal decomposition process, femtosecond laser energy is believed to be absorbed primarily by electrons (e.g. photon–electron interactions). This energy absorption and transfer takes place over picosecond timescales such that bonds are broken without heating the lattice (i.e. a disequilibrium process). Binding energies are thus overcome without significant heating of the lattice: the material 'explodes' into an aerosol composed of a mixture of atoms, ions, and small molecular fragments. As a result, inter-element fractionation from laser-target interactions is predicted to be negligible. This has obvious advantages for U-Pb geochronology. The significantly higher cost (currently) of turn-key femtosecond LA-ICP-MS systems (Photon Machines FS198.G2, NewWave Research NWR-femto, Allied Spectra J100) has limited their deployment to a relatively small cohort of institutions. In North America, there are only a handful of femtosecond LA-ICP-MS systems operated by Earth Sciences departments (University of Windsor, University of Wisconsin, UC Santa Barbara, and UC Berkeley) with other experimental systems housed and operated by physics and materials science departments.

There are, however, many other sources of inter-element fractionation within a LA-ICP-MS system independent of the laser instrumentation. These include: 1) deposition of material on the inner surfaces of the cell (e.g. upper window or walls); 2) fractionation in the sample tubing (e.g. gravitational settling and electrostatic processes); and 3) mass-fractionation in the ICP-MS plasma and the ion-optical system. Some of these processes are not time-dependent and

so can be compensated for by matrix-matched external standardization.

KEY DEVELOPMENTS: SENSITIVITY, SAMPLE CELLS, AND SOFTWARE CONTROL

Sensitivity

Changes to quadrupole-ICP-MS ion optical system and interface designs recently introduced by Agilent (e.g. 7700x), Thermo (X-SeriesII), Perkin-Elmer (NexION 300), and Bruker Daltonics (Aurora M90) have resulted in instruments with inherently higher sensitivity than previous generations. Additional steps can be taken to further enhance the sensitivity of LA-ICP-MS by changing the conditions of: 1) the 'dry' plasma, and 2) the vacuum in the interface region between the cones and the extraction lens. First, adding a small amount of high-purity H_2 or N_2 to the aerosol carrier gas can be used to significantly increase the temperature of the plasma and thereby enhance its ionizing efficiency (Guillong and Heinrich 2007). Other studies have recently shown that mixtures of high-purity CH_4 + Ar and CH_3OH (methanol) + Ar may have even larger effects on sensitivity enhancement (Fliegel et al. 2011), but this approach can also generate unwanted polyatomic interferences. Using N_2 has merit as it can be obtained at purities of the same level as the He carrier gas (e.g. 99.999%) and is inert but results in significantly increased nitride interferences. The amount of N_2 or other gas mixture required to maximize sensitivity varies from instrument to instrument. Typical flows for N_2 are between 2 to 5 mL/min added to the He + Ar carrier gas. Figure 2 shows the effect on ^{207}Pb intensity of adding 2.8 mL/min N_2 to an Agilent 7700x. These data were acquired under the same analytical conditions used for U-Pb geochronology of zircon. It should be noted that sensitivity on NIST610 *could* be significantly increased simply by increasing the laser fluence (e.g. to 8 J/cm^2), but this would compromise the goal of keeping ablation craters shallow for *in situ* work in thin sections. Notice that the robustness of the plasma (monitored as oxide production and U/Th ratio ≈ 1) remains high even under maximum sensitivity conditions. The much greater ionization efficiency under these conditions does enhance the production of doubly-charged species (more ions reach their second ionization potential), and may contribute to the formation of molecular ion interferences (e.g. possible ^{176}Hf^{14}N^{14}N interference on ^{204}Pb in zircon).

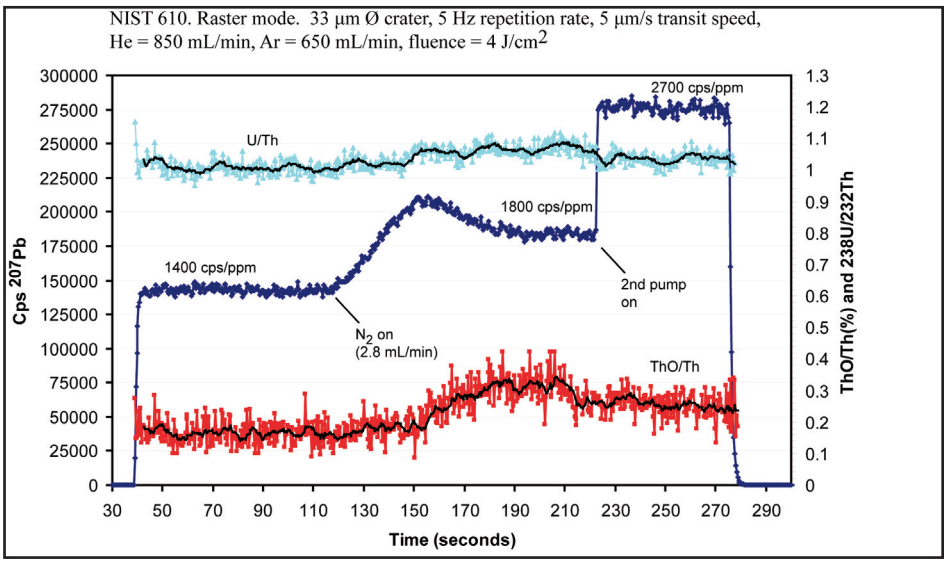

Figure 2. Effect on ^{207}Pb signal, oxide production (ThO/Th) and U/Th ratio of adding N_2 to the carrier gas mixture and increasing the interface region vacuum. Moving average shown in black for oxide production and U/Th data.

Another technique that can enhance sensitivity is the use of a larger interface rotary pump, or multiple rotary pumps, to increase the vacuum in the region between the sample cone and the first ion extraction lens. Thermo Scientific have introduced a similar upgrade for their magnetic-sector ICP-MS line called the 'Jet Interface' that features a larger 'dry' vacuum pump and redesigned cones (see, for example, Newman 2012). We use a manually controlled second external rotary pump that can be turned on to increase sensitivity of Pb and U. In Figure 2, the effect of turning the second rotary pump on is illustrated by the sharp jump in ^{207}Pb intensity. The effect is instantaneous because operating the second pump immediately lowers the pressure in the interface region from 2.3 ×10^{-2} kPa to 1.9 ×10^{-2} kPa on our Agilent 7700x ICP-MS. The combination of N_2 and second rotary pump allows us to obtain sensitivity as measured on the NIST610 silicate glass of ~2700 icps/ppm for ^{207}Pb at a spot diameter of 33 µm, pulse energy of 4 J/cm^2, and repetition rate of 5 Hz. The zircon 91500 standard contains only about 1 ppm ^{207}Pb such that under these analytical conditions we can achieve a net intensity of ~2500 icps for ^{207}Pb.

For U-Pb geochronology of young accessory minerals, such as titanite, rutile, and allanite, which can contain a significant common-Pb component (e.g. ^{207}Pb*/^{204}Pb^c <100), it may be necessary to quantitatively subtract the common-Pb component from each of the radiogenic daughter products. This is most accurately accomplished by direct measurement of the ^{204}Pb signal during ablation. The presence of trace-level impurities of Hg in the carrier gases (with ^{204}Hg isobarically interfering with ^{204}Pb) requires that Hg be either removed from the gas using impurity traps (e.g. gold-coated sand traps) or peak-stripped from the net mass 204 peak by monitoring ^{202}Hg and assuming an instrumental ^{204}Hg/^{202}Hg value. Even so, some authors (Simonetti et al. 2006) suspect the existence of additional polymolecular interferences on ^{204}Pb, casting doubt on the reliability of this approach. Alternatively, many labs simply ignore ^{204}Pb and rely on common-Pb corrections, such as the method proposed by Andersen (2002), which is based on the measured ^{208}Pb signal, U/Th ratio, an estimate of the age of the target, and the model common-Pb composition (e.g. Kramers

and Tolstikhin 1997). In the UNB lab, we use dedicated high-capacity (up to 20 L/min) Hg traps manufacturered by Vici Metronics on all of the gas lines that enter the laser and ICP-MS. These ensure that ^{204}Hg gas backgrounds remain <150 icps under the highest sensitivity conditions.

Sample Cells

The sample cell is arguably one of the most important components of any laser ablation system. The cell holds the samples and standards in a controlled atmosphere and presents the targets to the focused laser beam for ablation. Ideally, all ambient air must be removed from the cell (e.g. by repeated evacuation) and then continuously flushed with an ablation carrier gas (typically pure He or He + Ar). Aerosols generated during ablation should be fine grained, uniform in particle size distribution, and ideally be transported to the ICP-MS as quickly and efficiently as possible (fast cell washout and high sensitivity) with minimal contact with the cell walls or roof (which can cause additional inter-element fractionation). The conditions of aerosol generation and transport should also be identical anywhere in the cell to maximize its useable area. Whereas numerous custom-designed cells have been described in the literature, which are capable of fast washout or high sensitivity, commercially available cells come in two main configurations: 1) open cylindrical designs, and 2) two-volume cells. It is now widely documented that large-volume open cells can achieve fast washout and high sensitivity only for parts of the cell that lie between the inlet and outlet for the carrier gas. Transport of aerosol is efficient within this central channel, but inefficient and variable away from it, which limits the useful working area within these cells (Fisher et al. 2011; Koch and Gunther 2011). To circumvent the problem of maintaining constant washout and sensitivity throughout the cell, while also providing a large enough area to accommodate geologic samples (e.g. thin sections, polished slabs) and standards, two-volume low-volume (2VLV) cells have been developed. The most commonly used, the Australian National University (ANU) Helex design (Eggins et al. 1998) has been adopted by Resonetics (in collaboration within Laurin Technic Pty) and more recently by Photon Machines (e.g. Analyte G2 in collaboration with ANU Research School of Earth Sciences). A similar 'large format cell' was also developed by New Wave Research, but deployment of this cell has been limited. One of the principle benefits of the 2VLV cell is that ablation takes place within a low-volume (<1 cm^3) funnel, which can move around inside the cell (in the ANU Helex and Laurin Technic M-50 designs the cell actually moves around the funnel which is fixed). This ensures that ablation conditions, washout times, and transport efficiency are identical anywhere in the cell. The low-volume of the 2VLV design also ensures that aerosol washout is extremely fast (several orders of magnitude in <1 second). This means that background levels are re-established only a few seconds after the cessation of ablation, so that the next target in the sequence can be started almost immediately. This innovation significantly increases the number of analyses that can be conducted per hour. In a recent detrital zircon study using a Resonetics M-50-LR laser ablation system equipped with a Laurin Technic Pty 2VLV cell, 97 analyses (76 unknown zircons, 18 zircon standards, and 3 NIST glasses), each comprising a 15-second ablation followed by a 20-second washout period, were completed in just over 1 hour. The detrital zircons occur in a single, heavy-mineral layer in a thin section of tourmalinized metaquartzite from the lower Aldridge member of the Belt-Purcell basin west of Kimberley, BC. The results of this ablation sequence are shown in Figure 3.

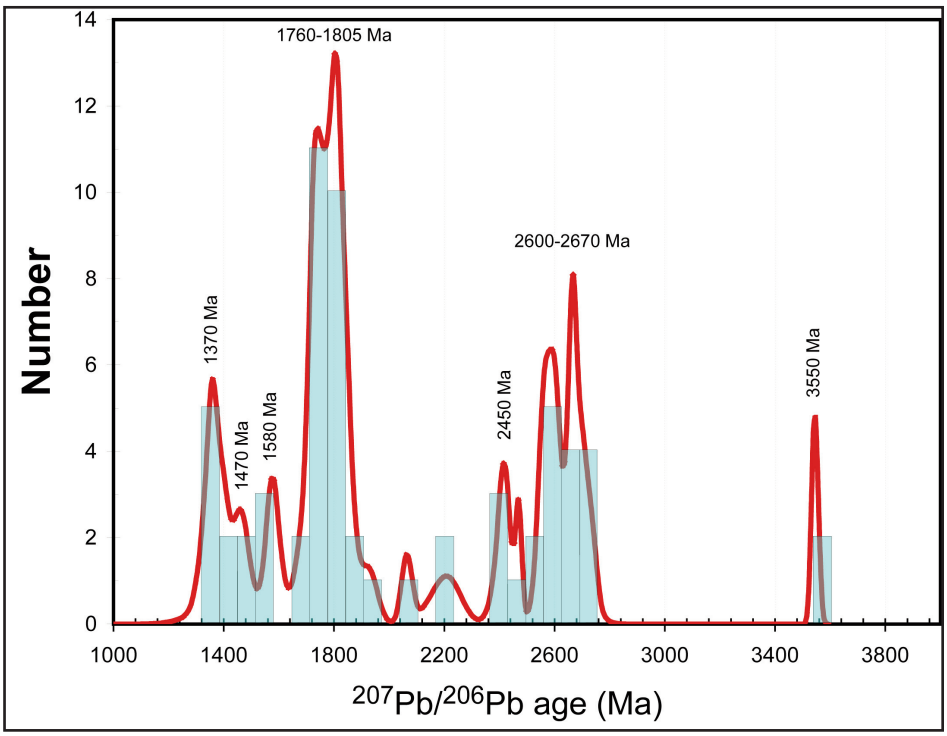

Figure 3. The rapid washout time of the 2VLV cell allows large datasets, such as this detrital zircon provenance curve, to be constructed in about 1 hour.

Signal Smoothing

The use of fast-washout sample cells with excimer-based lasers can lead to undesired oscillation of the time-resolved ICP-MS signal during ablation at repetition rates less than 4 Hz, when the transfer rate of aerosol from the cell (e.g. several orders of magnitude in <1 second) approaches that of the delay between pulses. Inline smoothing devices are, therefore, necessary to either lengthen or homogenize individual pulses prior to introduction to the ICP-MS torch. For example, the ANU Helex and Laurin Technic Pty designs use a high efficiency smoothing device called the 'squid' that first divides the

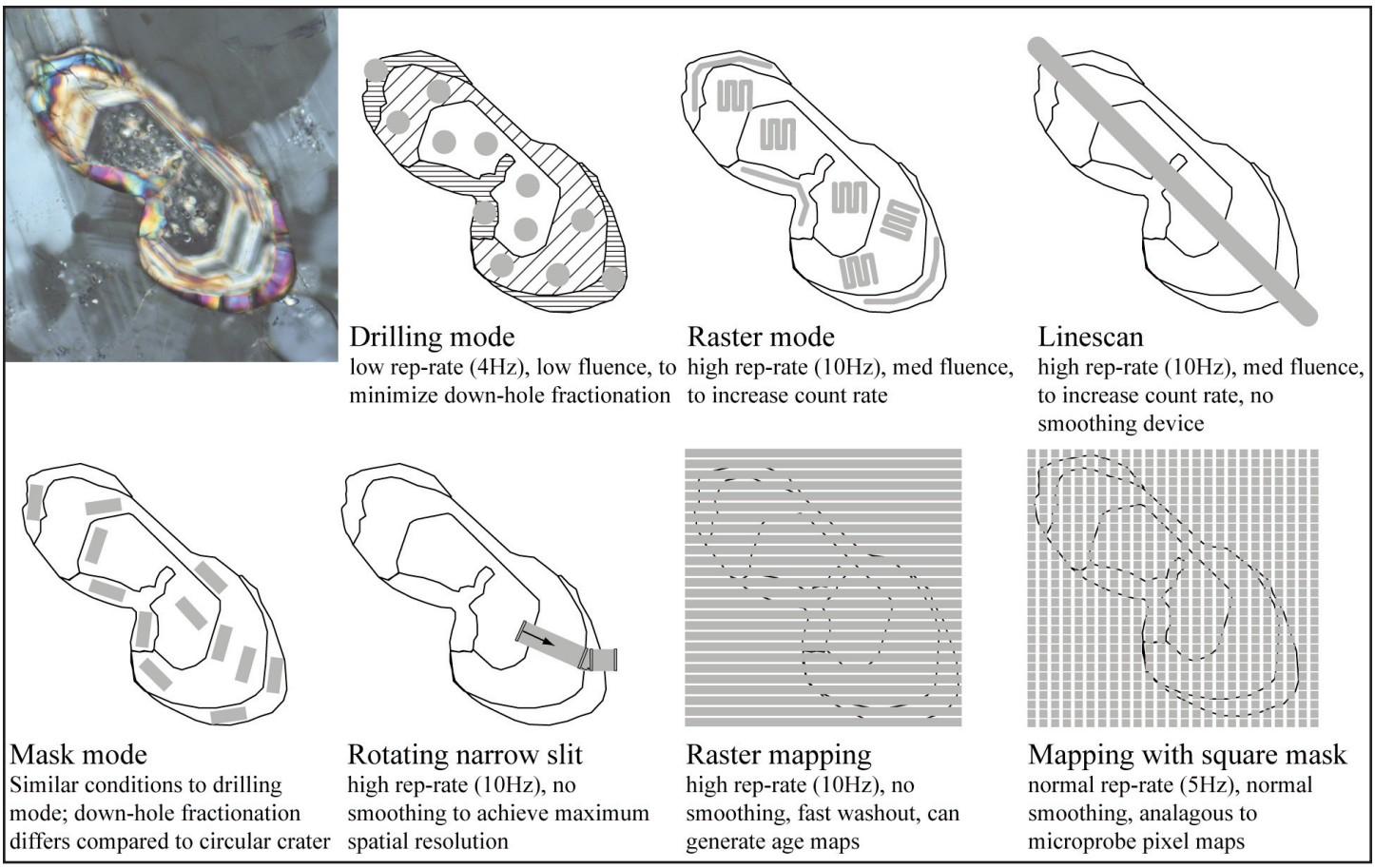

Figure 4. Ablation modes available on most new laser ablation systems. Depending on textural variations and compositional zoning within a target grain, different ablation modes can be used to target specific domains.

incoming aerosol gas stream into numerous different tubes each of different path length, and then recombines the separate paths into a 'stretched' output signal. Other manufacturers provide baffled cylindrical mixing bulbs designed to homogenize transient pulses before continuing on to the ICP-MS torch. Smoothing of this nature is critical for isotope measurements by single-collector-ICP-MS (either quadrupole or magnetic sector) in which ions are counted sequentially: significant variations in intensity (e.g. oscillating signal) during the measurements sequence (e.g. ^{238}U might be counted 0.1 seconds after ^{206}Pb) will lead to high internal errors that can compromise the final propagated precision. The importance of signal smoothing using the 'squid' is well illustrated by Müller et al. (2009). They also demonstrated a phenomenon known as spectral skew, which arises when the laser repetition rate and ICP-MS sampling time give rise to long-period (e.g. several second) oscillations or 'beating' of the signal. This spectral skew can be eliminated by changing either the ICP-MS dwell times or laser repetition rate.

Software Control

Ablation Modes and Ablation Timing

Laser ablation system control software has been engineered with synchronized stage motion, laser triggering, and laser pulse timing to facilitate a wide range of laser ablation techniques. The simplest application of this synchronization involves automated execution of large ablation sequences pre-programmed with crater diameter, laser energy, repetition rate, ablation duration and timing constraints for backgrounds and sample pre-cleaning operations. Figure 4 shows some of the wide variety of standard ablation modes typically available on modern laser ablation systems. The ability to mask the laser beam using narrow rectangular slits enables high spatial resolution linescans across compositional domains. The rotating rectangular slit available on the Resonetics system additionally enables synchronization between stage motion, laser firing, and rotation angle of the slit. This approach is used to ensure that the narrow direction of the slit is always parallel to the direction of travel, thereby yielding the highest possible spatial resolution.

Synchronization with ICP-MS

The recent development and dissemination of Iolite™ software (Paton et al. 2010, 2011) has allowed both manufacturers and end-users to change their approach to laser ablation. Iolite™ represents a significant departure from other widely used U-Pb data reduction schemes such as LAMDATE (Košler et al. 2002) and GLITTER™ (Griffin et al. 2008), in which data are processed on a spot-by-spot basis.

Iolite, which runs as a plugin in Wavemetrics Igor Pro 6.2x™, allows time-series data (e.g. cps vs. time for each analyte) for primary standards, quality control standards, and unknowns to be collected and reduced as a single output file that could represent several hours of continuous data collection. Such long acquisitions are not unusual for solution-based ICP-MS, where integrated autosamplers and pre-defined sequences are used to analyze large batches of liquid samples. Laser ablation system manufacturers have now adopted a similar approach, in which the user builds up a sequence of numerous, pre-defined ablations, which can be run automatically or semi-automatically (i.e. with user doing the final fine-positioning) while the ICP-MS collects data continuously over the same time interval. A time-lapse movie that shows a 20 minute ablation sequence in which Temora zircon was analyzed using zircon 91500 as a standard is available at:

http://youtu.be/EcR-JwYy-bo

The movie shows various modes of illumination, the growth of ablation blankets (visible in reflected light), and the plasma plume (with illumination off) that is generated within each laser pulse. At the end of the sequence, the laser software generates a .csv log file that records the laser 'on' and 'off' timestamps, which Iolite™ uses to synchronize with the ICP-MS output file. The laser log file also records all other variables as metadata, such as target labels, raster scan speed, repetition rate, laser energy, and cell pressure.

By synchronizing the laser control and ablation sequencing with the intensity data measured by the ICP-MS, Iolite™ can also be used to 'auto-integrate' the icps versus time data related to each type of ablation (e.g. standards, unknowns). For target grains that contain complex zoning, evidence for heterogeneous Pb-loss, or that require a common-Pb correction, VizualAge™ (Petrus and Kamber 2012) is used to manually select the intervals within the signal that yield either the most concordant data or the lowest internal errors on ratios such as $^{207}Pb/^{206}Pb$. The automatic integration feature also allows the definition of a continuous baseline for the entire analytical sequence. One of the numerous advantages of this approach is the ability to accurately correct for instrument drift (as recorded by time-dependent changes in the standards) and to use different splines to accurately model and subtract the gas background. The ability to accurately and rapidly reduce laser ablation data using two synchronized files (one from the laser and one from the ICP-MS) ensures that the results of each ablation sequence can be processed and inspected before the next batch of data is collected. This approach is not quite 'on-the-fly', but this could easily be achieved through increased collaboration between laser and ICP-MS instrument manufacturers.

Elemental Fractionation Corrections

Drilling mode analysis

Accurate and precise U-Pb geochronology using 193 nm ArF excimer LA-ICP-MS in 'drilling' mode is dependent on external standardization to correct for both LIEF at the ablation site, within the transport tubing connecting the laser cell and the ICP-MS, fractionation within the ICP-MS torch, and for mass-discrimination within the ICP-MS ion optical system. Testing the effectiveness of LIEF corrections is relatively straightforward. If a standard and unknown are sufficiently matrix-matched such they display similar LIEF, then application of the correction will yield constant $^{206}Pb/^{238}U$, $^{207}Pb/^{235}U$ and $^{208}Pb/^{232}Th$ as a function of time, assuming the unknown has a constant age within the volume of the crater. The power of Iolite™ software described above is its ability to fit different functions (e.g. linear, exponential, power law) to the measured LIEF for Pb/U and Pb/Th. The goodness-of-fit of different models can be easily assessed and, if necessary, customized functions can be implemented to best describe the fractionation relationship (Paton et al. 2010).

Once the standard and unknowns are corrected for LIEF, the difference in the measured versus true isotopic ratios for the standard arising from mass-discrimination induced by the ICP-MS are used to further correct the unknowns. These corrections can be significant (e.g. a few percent) for Pb/U and Pb/Th ratios because of the higher transmission efficiency through the ICP-MS ion optic system of U and Th relative to Pb. In contrast, the measured $^{207}Pb/^{206}Pb$ may differ by <1% compared to the true ratio because laser-induced fractionation of isotopes of the same element and mass-discrimination between mass 206 and 207 during transmission through the ICP-MS are minimal. Figure 5 shows how this process works for a monazite analyzed with a 45 μm crater in a sequence that was standardized against the Trebilcock monazite. The final corrected ratio overlaps with the known value as measured independently by SHRIMP.

Well characterized, matrix-matched standards exist for zircon (e.g. 91500, QGNG, Temora, FC-1) and baddeleyite (FC-1), but there are no well-characterized and widely distributed matrix-matched standards for most of the other accessory minerals that are routinely dated (i.e. monazite, titanite, allanite, apatite, perovskite, and rutile). In most cases, matrix-matched standards are developed in-house and their efficacy demonstrated by the reproduction of concordant ages on well-established quality control material. For example, the 416 Ma Temora zircon standard is commonly used to test the accuracy and precision of zircon U-Pb dating methods. A typical result for Temora analyzed on the University of New Brunswick LA-ICP-MS system is shown in Figure 6.

If the matrices do not exhibit comparable ablation characteristics (e.g. analyzing metamict zircon using a crystalline zircon standard) then normal and reverse discordance is likely to occur, as a result of mismatched Pb/U fractionation correction. In these cases, minimizing laser-induced fractionation by rastering would yield the most concordant results and many LA-ICP-MS labs adopt this approach.

In many cases, there are no matrix-matched standards that are suitable for LA-ICP-MS geochronology. This often arises for accessory minerals that contain significant amounts of common-Pb. In such cases, it is very difficult to find an isotopically homogeneous and concordant standard that can be used to make the corrections described above. A rare exception in

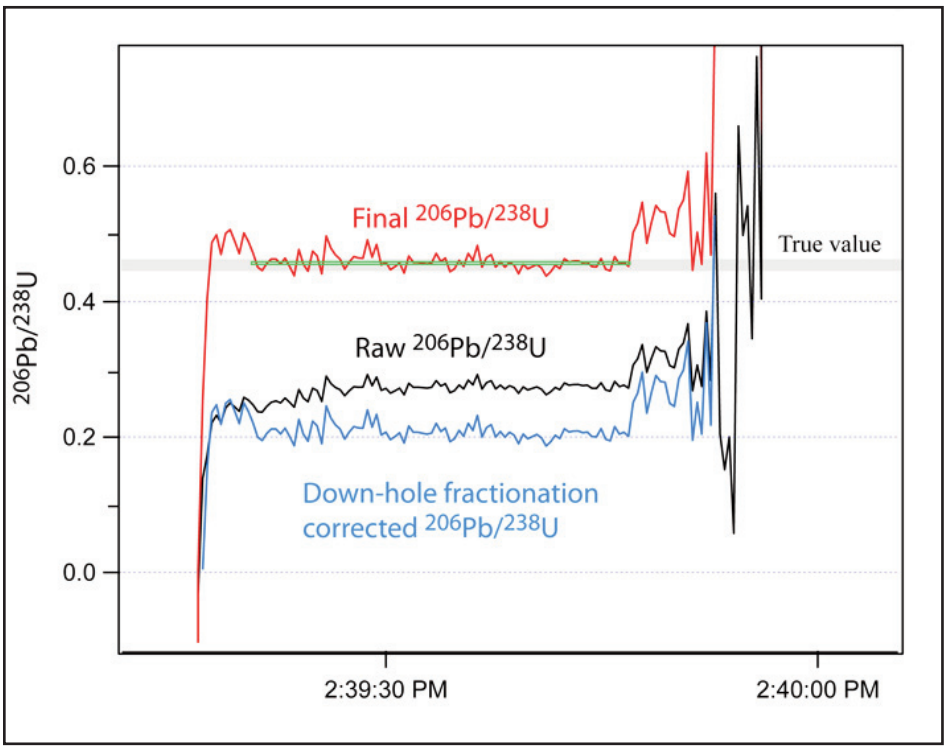

Figure 5. Raw, LIEF-corrected, and mass-discrimination-corrected time-series for $^{206}Pb/^{238}U$ ratio for a monazite unknown analyzed with a 45 μm crater in a sequence standardized using Trebilcock monazite. The green bar (the height of which in Iolite is proportional to the error) is the final integration period used to calculate the error for the final $^{206}Pb/^{238}U$ ratio.

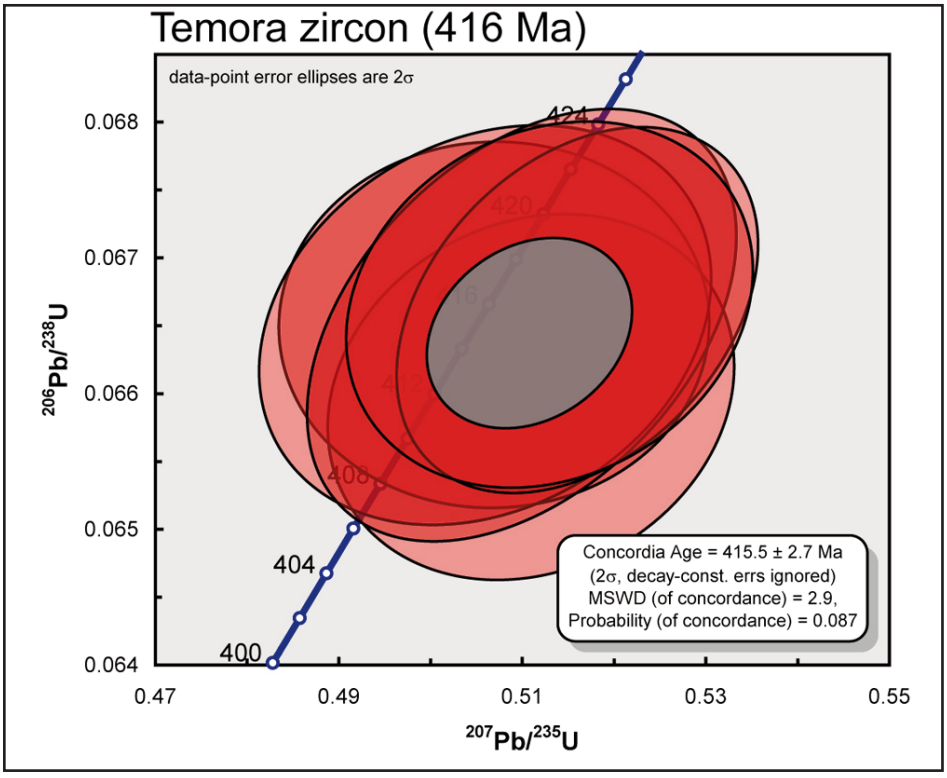

Figure 6. Results of a quality-control run on Temora zircon using a 24 μm diameter crater. The calculated Concordia age overlaps within error the true age, confirming the accuracy of the analytical method.

use at UNB and elsewhere is the ~520 Ma Khan Mine titanite, which was formed from a very high U/Pb source rock. No such standards currently exist for other common-Pb bearing minerals such as apatite and allanite.

Raster mode analysis

By using raster-mode ablation, thereby minimizing LIEF, it is usually possible to use matrix-*mis*matched standards to reliably correct for instrumental mass-discrimination. For example, Chew et al. (2011) have recently developed apatite dating methods using raster analysis that rely on zircon 91500 as an external standard. Zircon is used in preference to other potential standards because it shares similar absorbance to apatite and so both minerals ablate under similar fluence conditions.

Image Overlays

Laser ablation manufacturers now provide software interfaces that enable image files from other instruments to be overlain (e.g. as semi-transparent layers) on top of the basic video feed from the laser optical system. Internal zoning information in target materials recorded using polarizing microscopy, backscattered electron (BSE) imaging, cathodoluminescence imaging (CL), or compositional maps (from either the laser itself or from electron microbeam instruments), can be overlain in the laser software to help guide the placement of ablations in the sequence. This ability is particularly useful when analyzing complexly zoned accessory minerals that may contain several generations of inherited components.

The UNB laser ablation system is highly integrated with both SEM and optical imaging instruments. The principle imaging instrument is a Zeiss AxioImager, which is equipped with a motorized X-Y stage. This tool allows us to create seamless mosaics (using the AxioVision software 'Mosaix' routine) of entire thin sections or polished slabs, augmented when necessary by high magnification transmitted and reflected light images of the most important targets. Because the objectives are calibrated, the AxioImager is also used to measure the size of targets and to determine the diameter of the crater or raster pattern that can be used for each grain.

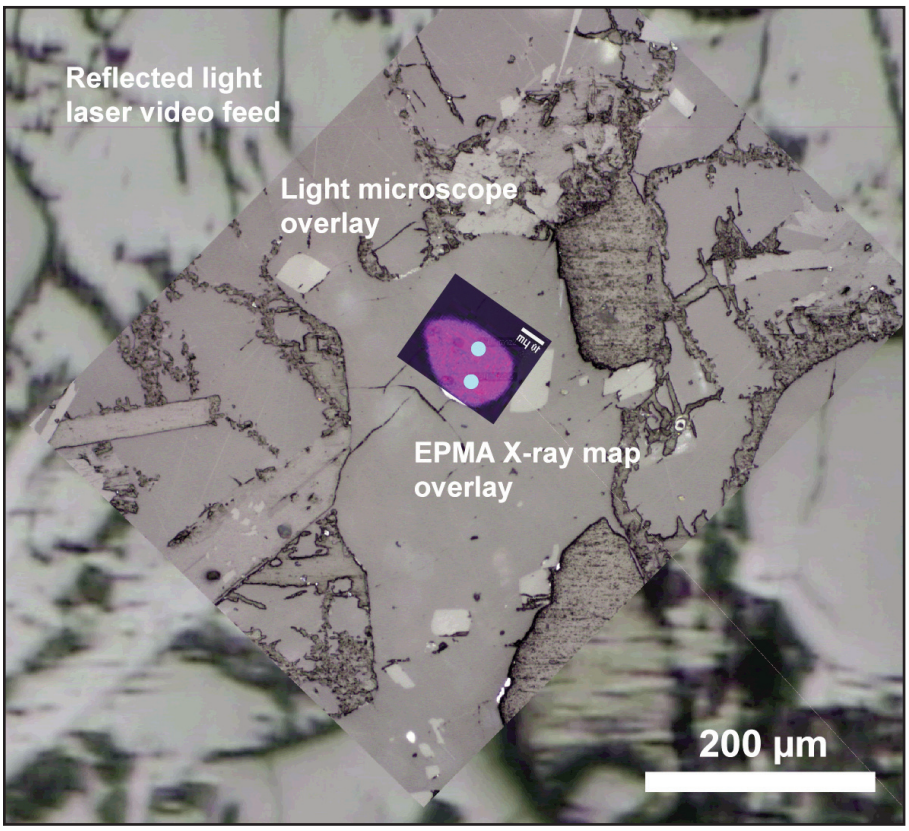

Figure 7. Example of multi-layer overlays at progressively higher levels of detail. This process is used to ensure the laser crater is positioned so as to sample uniform elemental or isotopic domains.

This ability to integrate different kinds of macro- and micro-imaging ensures that internal zoning features in accessory minerals can be identified and accurately targeted for LA-ICP-MS. Figure 7 shows two levels of image overlays that have been 'georeferenced' to the underlying laser system stage coordinates to help accurately position craters on a small monazite grain.

Offline Definition of Ablation Sequences

Some laser ablation system manufacturers (e.g. Resonetics) are also now producing 'offline' versions of their ablation software that allow users to construct ablation sequences prior to the actual analytical session. In this approach, images of the target area are first imported into the offline software, and the relative locations of ablation points, lines, paths, or polygons defined. The offline definition of these points can include such parameters as target labels, repetition rate, ablation time, etc. The image and the predefined ablation sequence are then saved as a single file. The combined image and its predefined ablation sequence are then imported into the online laser software at the start of an analytical session. Figure 8 shows a seamless mosaic of a zircon-rich heavy-mineral layer in a polished thin section. The relative X-Y position of pre-defined ablation targets and the sequence of analysis (connected by lines) are shown. The image and stored points are then 'georeferenced' to the laser system X-Y stage using the online software. The only remaining step is to define a series of standard ablations and verify the ICP-MS tuning. This approach significantly increases the number of samples that can be analyzed during an analytical session.

APPROACH AND APPLICATIONS TO *IN SITU* U-Pb GEOCHRONOLOGY

Increasing LA-ICP-MS sensitivity as described above facilitates dating most accessory minerals with 10s to

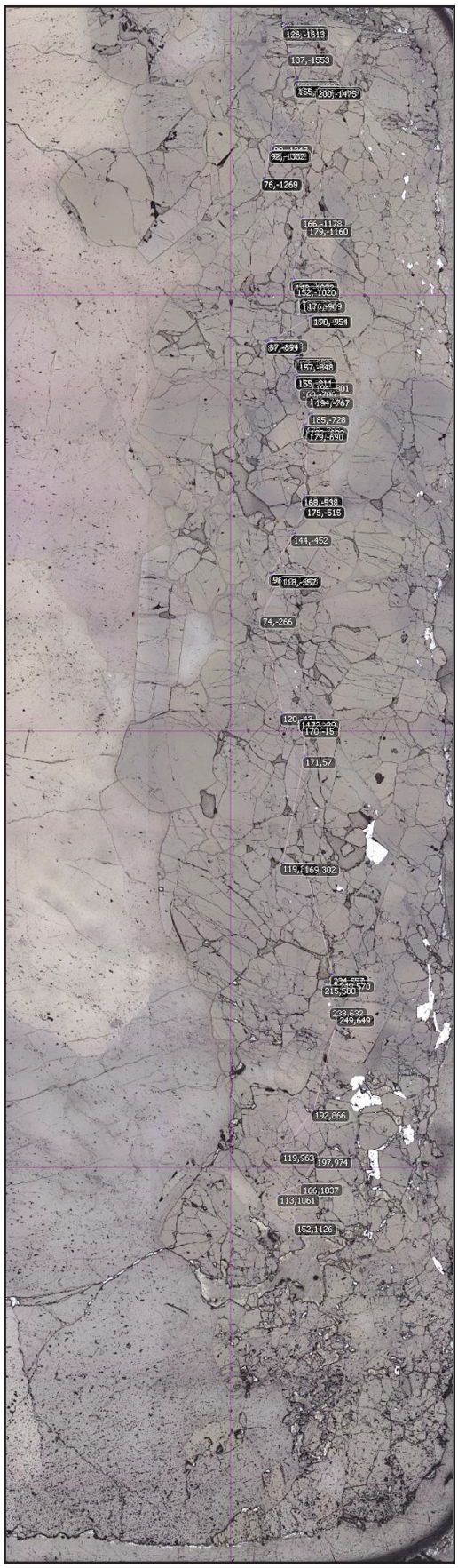

Figure 8. Offline ablation sequence defined for a heavy-mineral layer in a quartzite.

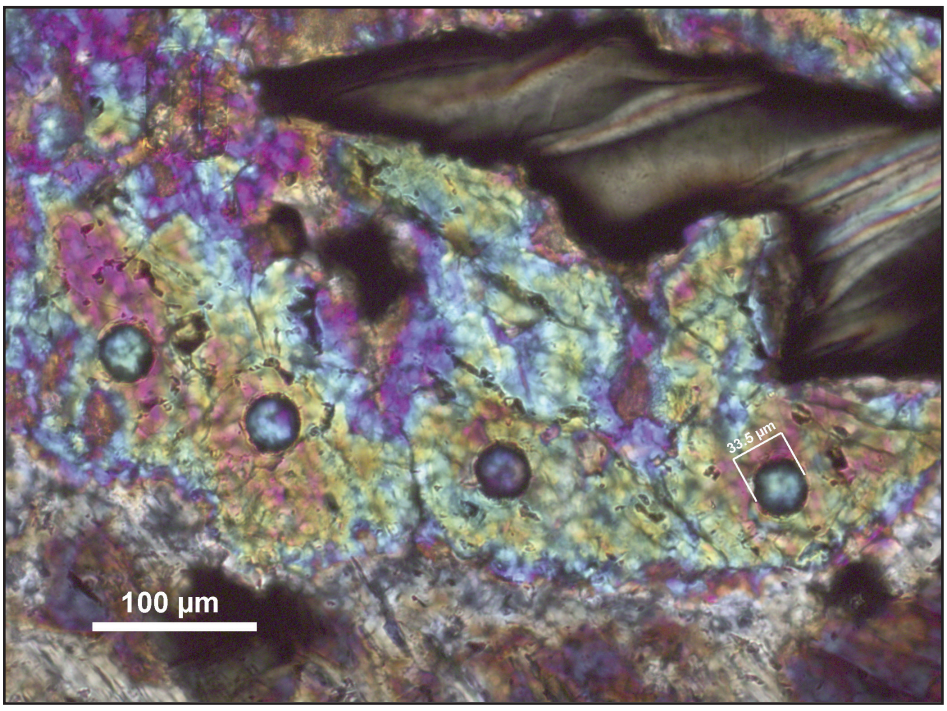

Figure 9. Adjusting ablation conditions (e.g. fluence and repetition rate) can be used to minimize crater depth, as shown here for 33 µm craters in epidote–allanite. The shift in interference colour from 2nd order pink to 2nd order blue-green is consistent with crater depths of 10 µm. The diameter of the crater was measured using our Zeiss AxioImager A1M polarizing microscope.

100s of ppm Pb and U concentrations using crater diameters <45 µm. Accessory minerals with higher U concentrations (e.g. 100s to 1000s of ppm U in monazite, allanite) can be successfully analyzed using craters <20 µm in diameter. In all cases, laser fluence and repetition rate can be optimized to ensure that craters are also half as deep as the diameter of the crater (i.e. depth/diameter ≤0.5). Figure 9 shows a crossed polarized photomicrograph of craters produced in epidote–allanite using a 33 µm diameter crater and 30 second ablation time at 4 Hz repetition rate. The decrease in interference colour between the top (2nd order pink) and bottom (2nd order blue-green) of the crater indicates depths of ~10 µm. This level of horizontal and vertical spatial resolution is critical for minimizing mixing between different age domains. Ablating shallow craters also helps reduce the magnitude of LIEF and, together with efficient sample smoothing, prevents the rapid loss of analyte intensity.

These ablation conditions are typically matched with an ICP-MS time-resolved analyse (TRA) method that takes advantage of the very fast peak-hopping capabilities of the quadrupole mass filter. For U-Pb geochronology, the dwell times (measured in ms) are typically: ^{207}Pb > ^{206}Pb > ^{208}Pb ≥ ^{232}Th ≥ ^{238}U. This order reflects: 1) the diminishing abundance of Pb isotopes; 2) the need to ensure that the ^{207}Pb/^{206}Pb ratio has the highest precision, and; 3) the higher absolute concentration and ion transmission through the ICP-MS of U and Th. Dwell times are typically 10-20 ms for ^{208}Pb, ^{232}Th, and ^{238}U and somewhat longer dwell times of 30-80 ms for ^{206}Pb, ^{207}Pb and ^{204}Pb (if the latter is even analyzed). The goal of this setup is to ensure that a single sweep of the quadrupole is almost instantaneous, that a large number of measurements per second are obtained, and that a sufficient number of ions are counted for each mass (see, for example, Halicz et al. 1996). Adding up individual dwell times plus quadrupole settling time (<1 ms) typically yields total integration times ≤0.25 seconds so that a 35 second ablation will yield ~140 independent measurements of the ^{207}Pb/^{206}Pb, ^{206}Pb/^{238}U and ^{208}Pb/^{232}Th ratios (^{207}Pb/^{235}U is calculated offline using the natural abundance of ^{235}U/^{238}U = 1/137.88).

Using this approach allows ArF excimer LA-ICP-MS to achieve short-term precision, expressed as relative standard deviation (%RSD) for the raw ^{207}Pb/^{206}Pb, ^{206}Pb/^{238}U, and ^{207}Pb/^{235}U in the range of 0.5 to 3.5% as shown in Table 1.

Precision on the final corrected ratios is typically better than shown in Table 1 because the data are corrected for instrument drift, and processing with Iolite™ and VizualAge™ helps refine the standard time integrations to achieve the most coherent population. The precision for the ^{207}Pb/^{206}Pb in this table was also optimized by using the longest dwell times for ^{207}Pb (75 ms)

Table 1. Precision, expressed as %RSD of raw ratios, for replicate analyses (*n*) of isotopically homogeneous standards at routinely used laser crater diameters and repetition rates (data obtained using Resonetics M-50-LR laser ablation system and Agilent 7700x ICP-MS).

Standard	Crater Ø (µm)	Rep. rate (Hz)	*n*	Ablation time (sec)	Raw ^{206}Pb/^{238}U (%RSD)	Raw ^{207}Pb/^{235}U (%RSD)	Raw ^{207}Pb/^{206}Pb (%RSD)
Khan Titanite (520 Ma)	45	4	13	30	0.55	0.76	0.55
91500 Zircon (1065 Ma)	24	4.5	18	35	0.87	1.04	0.84
Trebilcock Monazite (272 Ma)	14	4.5	16	30	1.36	1.76	1.04
FC-1 Zircon (1099 Ma)	10	4.5	14	30	3.08	3.34	2.24

Table 2. Typical workflow used for *in situ* LA-ICP-MS U-Pb geochronology of accessory minerals in standard 30 μm polished thin sections.

Creation (if necessary) of polished thin section scan or reflected-light mosaic and optical identification of accessory mineral targets. Estimation of largest crater diameter that can be used to analyze specific compositional domains.
↓
Backscattered electron (BSE) and/or cathodoluminescence (CL) imaging, electron microprobe X-ray mapping to identify textural and/or compositional domains.
↓
Online or offline definition of ablation sequence (e.g., ~30-50 unknowns, 15 standards, quality control material). Use image overlays if necessary for complexly-zoned target grains.
↓
Data acquisition using supervised semi-automatic ablation: for very small craters (e.g., 14 μm) user does final fine-positioning of crater since most X-Y stages have 2-4 μm reproducibility.
↓
Data reduction using Iolite™ and VizualAge™ while the next sample in the analytical session is queued.
↓
Data output and assessment of accuracy using quality control standards (e.g., Temora, RS33 zircon; Thompson Mine, 44069 monazite).
↓
Check craters optically and correlate measured U-Pb ages with textural or compositional domains.

and ^{206}Pb (30 ms) thereby ensuring that error ellipses on a conventional Concordia diagram have positive error correlations and can be plotted using Isoplot (Ludwig 2003). Assuming that ICP-MS sensitivity is maximized as described above and that 1% RSD on the raw $^{207}Pb/^{206}Pb$ is a reasonable minimum precision, the data in Table 1 also demonstrates that there are limits to crater diameters useable on different accessory minerals which is a function of absolute U concentration and age for the standard. For example, zircon can be analyzed with minimum crater diameters between 24 μm (using 91500) and 20 μm (using higher-U FC-1 as a standard) whereas similar precision can be achieved on monazite using 15 to 20 μm diameter craters owing to its significantly higher U and Pb* concentration.

Typical workflow for *in situ* U-Pb accessory mineral geochronology using the methods described above is shown in Table 2.

CONCLUSIONS

By combining enhanced ICP-MS sensitivity, fast and efficient sample cells, and sophisticated software controls, modern 193 nm ArF excimer LA-ICP-MS systems are able to:

1) Obtain precise and accurate U-Pb isotope data at crater sizes < 45 μm in diameter and <20 μm deep for most accessory minerals, facilitating *in situ* analyses in standard 30 μm thick polished thin sections.
2) Use low repetition rates to maintain shallow craters, thereby minimizing LIEF, and reducing the effects of matrix mismatches between standards and unknowns. This not only leads to increased accuracy and precision, but has also enabled development of U-Pb dating protocols for a wider range of accessory minerals.
3) Identify ablation targets and define ablation sequences offline, thereby increasing the overall efficiency and cost-effectiveness of the technique.
4) Seamlessly integrate internal zoning information captured using combinations of polarizing microscopy, SEM-BSE, SEM-CL, EPMA X-ray elemental maps.
5) Rapidly reduce and inspect results using Iolite™ and VizualAge™ software to confirm the precision and accuracy of LA-ICP-MS analytical conditions and assess the need for further refinement of ages.

ACKNOWLEDGEMENTS

The authors are grateful to S. Jackson and J. Gagnon for their thoughtful review of the original manuscript. We would also like to thank M. Hamel (Resonetics LLC) for his technical support over the duration of this project. The UNB laser ablation lab (with co-PIs D. Lentz and C. Shaw) was built with the support of the CFI Leaders Opportunity Fund, NBIF Research Innovation Fund, Xstrata Zinc, M. Watson, Elmtree Resources, NB Department of Natural Resources and with in-kind support from Resonetics LLC and Agilent Technologies Canada. Y. Luo was additionally supported by a NBIF Research Assistantships Initiative grant. A portion of this research was also supported by an NSERC Discovery Grant to C.R.M.M.

REFERENCES

Andersen, T., 2002, Correction of common lead in U-Pb analyses that do not report 204Pb: Chemical Geology, v.192, p. 59-79, http://dx.doi.org/10.1016/S0009-2541(02)00195-X.

Basting, B., and Marowsky, G., 2005.

Excimer Laser Technology: Springer-Verlag, Berlin, 433 p., http://dx.doi.org/10.1007/b137894.

Becker, J.S., 2002, State-of-the-art and progress in precise and accurate isotope ratio measurements by ICP-MS and LA-ICP-MS: Journal of Analytical Atomic Spectrometry, v.17, p. 1172-1185, http://dx.doi.org/10.1039/b203028b.

Chew, D.M., Sylvester, P.J., and Tubrett, M.N., 2011, U-Pb and Th-Pb dating of apatite by LA-ICPMS: Chemical Geology, v. 280, p. 200-216, http://dx.doi.org/10.1016/j.chemgeo.2010.11.010.

Cocherie, A., and Robert, M., 2008, Laser ablation coupled with ICP-MS applied to U-Pb zircon geochronology: A review of recent advances: Gondwana Research, v.14, p. 597-608, http://dx.doi.org/10.1016/j.gr.2008.01.003.

Darling, J.R., Storey, C.D., and Engi, M., 2012,Allanite U-Th-Pb geochronology by laser ablation ICPMS: Chemical Geology, v. 292-293, p. 103-115, http://dx.doi.org/10.1016/j.chemgeo.2011.11.012.

Eggins, S.M., Kinsley, L.P.J., and Shelley, J.M.G., 1998, Deposition and element fractionation processes occurring during atmospheric pressure laser sampling for analysis by ICP-MS: Applied Surface Sciences, v. 127-129, p. 278-286, http://dx.doi.org/10.1016/S0169-4332(97)00643-0.

Fisher, C.M., McFarlane, C.R.M., Hanchar, J.M., Schmitz, M.D., Sylvester, P.J., Lam, R., and Longerich, H.P., 2011. Sm-Nd isotope systematics by laser ablation-multicollector-inductively coupled plasma mass spectrometry: Methods and potential natural and synthetic reference materials: Chemical Geology, v. 284, p. 1-20, http://dx.doi.org/10.1016/j.chemgeo.2011.01.012.

Fliegel, D., Frei, C., Fontaine, G., Hu, Z., Gao, S., and Günther, D., 2011, Sensitivity improvement in laser ablation inductively coupled plasma mass spectrometry achieved using a methane/argon and methanol/water/argon mixed gas plasma: Analyst, v. 136, p. 4925-4934, http://dx.doi.org/10.1039/c0an00953a.

Gregory, C.J., Rubatto, D., Hermann, J., Berger, A., and Engi, M., 2012, Allanite behaviour during incipient melting in the southern Central Alps: Geochimica et Cosmochimica Acta, v. 84, p. 433-458, http://dx.doi.org/10.1016/j.gca.2012.01.020.

Griffin, W.L., Powell, W.J., Pearson, N.J., and O'Reilly, S.Y., 2008, GLITTER: data reduction software for laser ablation ICP-MS, in Sylvester, P., ed, p. 204-207 Appendix 2. Mineralogical Association of Canada Short Course Series Volume 40, Vancouver, BC.

Guillong, M., and Heinrich, C.A., 2007, Sensitivity enhancement in laser ablation ICP-MS using small amounts of hydrogen in the carrier gas: Journal of Analytical Atomic Spectrometry, v. 22, p. 1488-1494, http://dx.doi.org/10.1039/b709489b.

Guillong, M., Horn, I., and Günther, D., 2003, A comparison of 266 nm, 213 nm and 193 nm produced from a single solid state Nd:YAG laser for laser ablation ICP-MS: Journal of Analytical Atomic Spectrometry, v. 18, p. 1224-1230, http://dx.doi.org/10.1039/b305434a.

Halicz, L., Erel, Y., and Vernon, A., 1996, Lead isotope ratio measurements by ICP-MS: accuracy, precision, and long-term drift: Atomic Spectroscopy, v. 7(5), p. 186-189.

Koch, J., and Gunther, D., 2011, Review of the state-of-the-art of laser ablation inductively coupled plasma mass spectrometry: Applied Spectroscopy, v. 65, p. 155A-162A, http://dx.doi.org/10.1366/11-06255.

Košler, J., Fonneland, H., Sylvester, P., Tubrett, M., and Pedersen, R.-B., 2002, U-Pb dating of detrital zircons for sediment provenance studies - a comparison of laser ablation ICPMS and SIMS techniques: Chemical Geology, v.182, p. 605-618, http://dx.doi.org/10.1016/S0009-2541(01)00341-2.

Kramers, J.D., and Tolstikhin, I.N., 1997, Two terrestrial lead isotope paradoxes, forward transport modeling, core formation and the history of the continental crust: Chemical Geology, v. 139, p. 75-110, http://dx.doi.org/10.1016/S0009-2541(97)00027-2.

Liu, Z., Wu, F., Guo, C., Zhao, Z., Yang, J., and Sun, J., 2011, *In situ* U-Pb dating of xenotime by laser ablation (LA)-ICP-MS: Chinese Science Bulletin, v. 56, p. 2948-2956, http://dx.doi.org/10.1007/s11434-011-4657-y.

Ludwig, K.R., 2003, Isoplot 3.00: A Geochronological Toolkit for Microsoft Excel. Berkeley Geochronological Centre Special Publication no. 4, 70 p.

Müller, W., Shelley, M., Miller, P., and Broude, S., 2009, Initial performance metrics of a new custom-designed ArF excimer LA-ICPMS system coupled to a two-volume laser ablation cell: Journal of Analytical Atomic Spectrometry, v. 24, p. 209-214, http://dx.doi.org/10.1039/b805995k.

Newman, K., 2012, Effects of the sampling interface in MC-ICP-MS: Relative elemental sensitivities and non-linear mass dependent fractionation of Nd isotopes: Journal of Analytical Atomic Spectrometry, v. 27, p. 63-70, http://dx.doi.org/10.1039/c1ja10222b.

Pal, D.C., Chaudhuri, T., McFarlane, C., Mukherjee, A., and Sarangi, A.K., 2011, Mineral Chemistry and In Situ Dating of Allanite, and Geochemistry of Its Host Rocks in the Bagjata Uranium Mine, Singhbhum Shear Zone, India - Implications for the Chemical Evolution of REE Mineralization and Mobilization: Economic Geology, v. 106, p. 1155-1171, http://dx.doi.org/10.2113/econgeo.106.7.1155.

Paton, C., Woodhead, J.D., Hellstrom, J.C., Hergt, J.M., Greig, A., and Maas, R., 2010, Improved laser ablation U-Pb zircon geochronology through robust downhole fractionation correction: Geochemistry, Geophysics, Geosystems, v. 11, Q0AA06, http://dx.doi.org/10.1029/2009GC002618.

Paton, C., Hellstrom, J., Paul, B., Woodhead, J., and Hergt, J., 2011, Iolite: Freeware for the visualisation and processing of mass spectrometric data: Journal of Analytical Atomic Spectrometry, v. 26, p. 2508-2518, http://dx.doi.org/10.1039/c1ja10172b.

Petrus, J.A., and Kamber, B.S., 2012, VizualAge: A Novel Approach to Laser Ablation ICP-MS U-Pb Geochronology Data Reduction: Geostandards and Geoanalytical Research, v. 36, p. 247-270, http://dx.doi.org/10.1111/j.1751-908X.2012.00158.x.

Simonetti, A., Heaman, L.M., Chacko, T., and Banerjee, N.R., 2006, In situ petrographic thin section U-Pb dating of zircon, monazite, and titanite using laser ablation-MC-ICP-MS: International Journal of Mass Spectrometry, v. 253, p. 87-97, http://dx.doi.org/10.1016/j.ijms.2006.03.003.

Sylvester, P., 2001, Laser-Ablation-ICPMS in the Earth Sciences: Principles and Applications. In R. Raeside, Ed. Mineralogical Association of Canada

Short Course Series Volume 29. Mineralogical Association of Canada, St. John's, NFLD, 243 p.
Sylvester, P ., 2008, Laser Ablation ICP-MS in the Earth Sciences: Current Practices and Outstanding Issues. In R. Raeside, Ed. Mineralogical Association of Canada Short Course Series Volume 40. Mineralogical Association of Canada, Vancouver, BC, 356 p.
Zack, T., Stockli, D.F., Luvizotto, G.L., Barth, M.G., Belousova, E., Wolfe, M.R., and Hinton, R.W., 2011, In situ U-Pb rutile dating by LA-ICP-MS: ^{208}Pb correction and prospects for geological applications: Contributions to Mineralogy and Petrology, v. 162, p. 515-530, http://dx.doi.org/10.1007/s00410-011-0609-4.

Received June 2012
Accepted as revised June 2012